

2

Fundamentals of Stress and Strain at the Nanoscale Level: Toward Nanoelasticity

Pierre Müller

2.1

Introduction

Understanding the relationship between the structure and the shape of a piece of matter and its mechanical properties has always been one of the primary goals of material science. Over the past decades, the rapid progress in the development of new materials with a size of a few nanometers has opened a new field of scientific and technological interest. From a fundamental viewpoint, one of the key features of nanosized material is their high surface/bulk ratio with the consequence that materials in small dimensions behave differently from their bulk counterpart. From a technological viewpoint, nanomaterials are promising building blocks in future devices, but the stresses they develop can be detrimental to their reliability or can be used to modify their physical properties. Thus, for both fundamental and technological applications, there is a growing interest in the study of the mechanics of nanosized objects.

For instance, it has been found that the elastic modulus, which measures the proportionality between the applied stress and the measured strain, is size dependent for dimension smaller than roughly 200 nm. However, according to the authors, calculated or measured elastic moduli have been reported to increase or decrease with the size of the object. From an experimental viewpoint, this discrepancy may come from the difficulty of manipulation and the lack of characterization of such small objects, as well as from the uncertainty of the complex boundary conditions between a nanosized object and the micronic-sized tool used to measure its elastic properties.

From a theoretical viewpoint, there are still some difficulties to perfectly describe elasticity at the nanoscale. Most of the models used for describing the mechanical properties of a body are based on the classical linear and infinitesimal theory of elasticity of continuum mediums [1, 2]. In such models, a macroscopic object is considered as a continuum medium, the surface of which is a simple boundary at which external forces are applied. It means that the classical macroscopic theory ignores surface effects since it does not attribute any specific elastic properties to the surface. However, because of the missing bonds, there is a redistribution of

electronic charges close to the surface that modifies the local binding properties so that the surface layers cannot have the same elastic properties as the underlying bulk. This means that because of the reduced coordination of surface atoms, a small piece of matter cut in a homogeneous body is not homogeneous. The simpler way to describe this inhomogeneity is to divide the object into a bulk core and a surface zone with different elastic properties. We will show that when such specific surface properties are considered, the elastic behavior of a finite-size body results from a subtle interplay between its bulk and surface properties and thus depends on the absolute size of the object.

Our goal in this chapter is to describe the elastic properties of nanoscale objects from the point of view of surface physicists. In other words, our purpose is to properly introduce surface effects on elastic classical theory.¹⁾ This chapter is divided into two parts. The first part emphasizes the theoretical background. It begins by a few results valid for the bulk (Section 2.2.1), followed by a description of the surface elastic properties (Section 2.2.2) in the Gibbs meaning (Section 2.2.3) and then in the two-phase models (Section 2.2.4). The second part concerns applications. We will describe how surface stress may induce spontaneous deformation of nanoparticles (Section 2.3.1), may modify the effective modulus of freestanding thin films (Section 2.3.2), and may play a role for the static bending of thin films (Section 2.3.3) and nanowires (Section 2.3.4). A short conclusion will sum up the main effects the surfaces induce on the elastic properties of nanoscale objects.

Again, our goal is not to review all recent results, since in particular the number of papers devoted to the study of the mechanical properties of nanosized objects is increasing exponentially, but essentially to underline the fundamentals of nanoelasticity.

2.2 Theoretical Background

2.2.1 Bulk Elasticity: A Recall

The classical theory of elasticity treats solids as continuum mediums in which the deformation is described by continuum fields such as the displacement vector $\vec{u}(\vec{r})$ and the strain tensor $\varepsilon(\vec{r})$, while internal forces are described by the stress tensor $\sigma(\vec{r})$. Within linear infinitesimal elasticity, the equilibrium deformation field is a solution of a second-order equation that has to be solved with boundary equations expressed in terms of external forces applied at the free surface of the body.

In this section, we will recall some classical results valid for bulk elasticity but necessary as a prerequisite before studying surface elasticity in Section 2.2.2.

1) The limit of the description is that it is necessary to be able to discriminate surface from bulk. Such models thus cannot be used to describe the elastic properties of aggregates formed only by a few atoms, for which it is no more possible to attribute to the atoms a surface or a bulk character.

2.2.1.1 Stress and Strain Definition

If a continuum medium is strained, a point in the body is displaced from its initial position \vec{r} to $\vec{r}' = \vec{r} + \vec{u}$. The vector \vec{u} of components $u_i = x'_i - x_i$ is called the displacement vector. The distance $d\ell = \sqrt{dx_1^2 + dx_2^2 + dx_3^2}$ between two points of infinitesimal vicinity $d\vec{x}$ before deformation becomes $d\ell' = \sqrt{dx_1'^2 + dx_2'^2 + dx_3'^2}$ with $dx'_i = dx_i + du_i$ after deformation. For small displacements, this distance can be written as $d\ell'^2 = d\ell^2 + 2\sum_{i,j}\varepsilon_{ij}dx_id x_j$, where the quantity

$$\varepsilon_{ij} = \frac{1}{2} \left(\frac{\partial u_i}{\partial x_j} + \frac{\partial u_j}{\partial x_i} \right) \quad (2.1)$$

is called the bulk strain tensor.

When the body is strained, there develop forces tending to restore its initial configuration. These internal forces are transmitted across the surface that bounds the volume. The forces \vec{F} dS exerted on the faces of an elemental cube centered on the considered point can be written for a face i as [1, 2]

$$F_i = \sum_j \sigma_{ij} n_j \quad (2.2)$$

where σ_{ij} are the components of the so-called stress tensor and \vec{n} is a unit vector directed toward the exterior of the face i (see Figure 2.1).

Notice that in the framework of infinitesimal elasticity, the stress and strain definitions do not make a distinction between the deformed and the nondeformed configuration of the body. This is not the case for large deformation [1, 2].

2.2.1.2 Equilibrium State

From Eq. (2.2), the force component F_i ($i = 1, 2, 3$) on a volume V bounded by a surface S is $F_i = \oint \sum_j \sigma_{ij} n_j dS$. It can be transformed into a volume integral

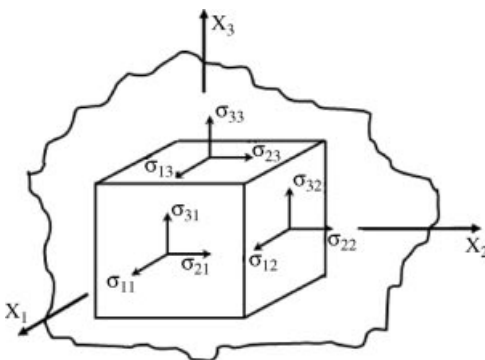


Figure 2.1 Action of the components σ_{ij} of the bulk stress tensor applied on the three front faces of an elementary cube cut in a piece of matter. Each face normal to x_j axis bears a triplet

σ_{ij} . The first index $i = 1, 2, 3$ gives the direction x_i where the stress acts. On the back faces of the cube, there are identical stresses of opposite sign.

$F_i = \int \sum_j (\partial \sigma_{ij} / \partial x_j) dV$, and so taking into account the Newton's second law $F_i = \int \rho (d^2 u_i / dt^2) dV$ (valid for a body of density ρ), we get

$$\sum_j \frac{\partial \sigma_{ij}}{\partial x_j} = \rho \frac{d^2 u_i}{dt^2} \quad (2.3)$$

which is called the elastodynamic equation.

At equilibrium, it reads

$$\sum_j \frac{\partial \sigma_{ij}}{\partial x_j} = 0 \quad (2.4)$$

Note that we have neglected all forms of body forces.²⁾

2.2.1.3 Elastic Energy

Under the action of external forces \vec{F} applied to the surface S of an elastic body of volume V , the surface points are displaced by $\delta \vec{u}$, so the work of the external forces is $\delta W = \oint \vec{F} \delta \vec{u} dS$. Using the expression of F_i given in Eq. (2.2), we have $\delta W = \oint \sum_j \sigma_{ij} n_j \delta u_i dS$. This surface integral can be transformed into a volume integral by means of the divergence theorem, so from Eqs (2.1) and (2.4), we have

$$\delta W = \int \sum_{i,j} \sigma_{ij} \delta \varepsilon_{ij} dV + \int \rho \frac{d^2 u_i}{dt^2} \delta u_i dV \quad (2.5)$$

The first part of (2.5) is the elastic contribution due to the elastic deformation and the second part is the variation of the total kinetic energy during the time dt .

We will denote bulk elastic energy by

$$\delta W^{\text{bulk}} = \int \sum_{i,j} \sigma_{ij} \delta \varepsilon_{ij} dV \quad (2.6)$$

2.2.1.4 Elastic Constants

In linear elastic theory, each stress component is assumed to be proportional to each strain component. Taking into account the tensorial nature of both strain and stress fields, this linear dependence (Hooke's law) can be written as

$$\sigma_{ij} = \sum_{k,l} C_{ijkl} \varepsilon_{kl} \quad (2.7)$$

where the material constants C_{ijkl} are called elastic (or stiffness) constants.

2) Body forces are proportional to the body mass. They include gravitational forces, magnetic forces, and inertial forces. They can be written as a volume integral over the body. In contrast, in the context of the classical elastic theory, surface forces result only from the physical contact of the body with another body and are thus expressed as a surface integral over the whole area of the body.

Using (2.7), after integration with respect to strain, Eq. (2.6) becomes

$$\delta W^{\text{bulk}} = \frac{1}{2} \int \sum_{i,j,k,l} C_{ijkl} \varepsilon_{ij} \varepsilon_{kl} dV \quad (2.8)$$

Depending on the crystal symmetry, one can further reduce the number of elastic constants. The maximum number of elastic constants is required for triclinic crystals, where it is 21. For isotropic bodies, it is 2. In this latter case, Hooke's law reads

$$\sigma_{ij} = \lambda \sum_k \varepsilon_{kk} \delta_{ij} + 2\mu \varepsilon_{ij} \quad \text{or} \quad \sigma_{ij} = \frac{E}{1+\nu} \left(\varepsilon_{ij} + \frac{\nu}{1-2\nu} \sum_k \varepsilon_{kk} \delta_{ij} \right) \quad (2.9)$$

when using the Lamé (λ and μ) or Hooke (E and ν) constants, respectively.

Note that the dilatation of a isotropic cube, uniformly loaded by pressure P , is

$$\sum_k \varepsilon_{kk} = -\frac{3(1-2\nu)}{E} P$$

where $K = E/3(1-2\nu)$ is the bulk elastic modulus.

2.2.2

How to Describe Surfaces or Interfaces?

In classical elastic theories of the previous section, surfaces solely serve to define boundary conditions but have no specific properties. In Section 2.2.3, we will see that as any extensive thermodynamic potentials (e.g., U , F , G , etc.), the elastic energy can be seen as a contribution from two homogeneous phases plus an interfacial term that contains all the elastic properties of the interfacial zone. The localization and the description of this interfacial zone are discussed in this section.

Consider a slab of thickness e in which, because of the missing bonds at the surface, any extensive quantity must continuously vary with the altitude z (see Figure 2.2). The central problem is how to discriminate bulk from surface contributions.

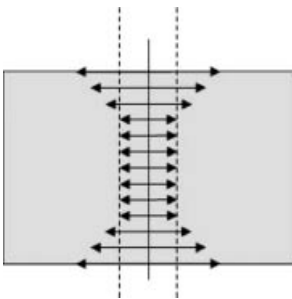


Figure 2.2 A slab of thickness e in which an extensive quantity continuously varies with the altitude. The extensive quantity (let us say a stress parallel to the surface) is represented by a double array whose length varies when approaching each surface.

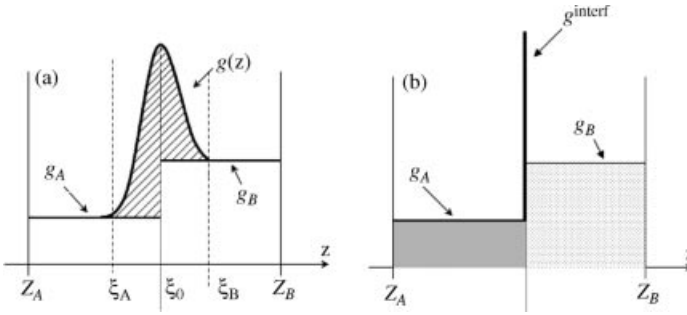


Figure 2.3 At the interface between two materials, A and B, extensive quantities are modified from their bulk values by an excess amount $g(z)$ (shaded) owing to the presence of

the interface (Figure 2.3a). In the Gibbs model, the whole excess quantity will be ascribed to the dividing surface separating two bulk materials (Figure 2.3b).

A first approach uses the concept of excess quantity [3]. More generally, let us consider two homogeneous phases A and B separated by a planar interface S_{AB} and let us consider an extensive quantity G whose density $g(z)$ varies across the interface (z is the axis perpendicular to the interface). In the bulk, far from the interface, g -profile is homogeneous. The interface modifies g by an excess quantity that corresponds to the shaded area in Figure 2.3a. The so-defined excess quantities is

$$g^{\text{interf}} S_{AB} = S_{AB} \left[\int_{z_A}^{z_B} g(z) dz - g_A(\xi_0 - z_A) - g_B(z_B - \xi_0) \right] \quad (2.10)$$

where g_i are the bulk density in each phase ($i = A, B$), S_{AB} the interfacial area, and g^{interf} the interfacial excess quantity per unit interface area. This definition does not depend upon the values of z_A and z_B provided they are, respectively, lower and higher than ξ_A and ξ_B .

Some well-known interfacial excess quantities are the number of particles in excess at the surface, the surface entropy, or even the mass excess of the interfacial zone. Gibbs [3] proposed, for a pure substance in contact with the vacuum, to choose the localization of the dividing surface ξ_0 to the mathematical plane for which there is no surface excess of mass³⁾ (Figure 2.4). In the case of a multicomponent substance, the dividing surface can be fixed to the mathematical plane for which the surface excess mass of one species is zero. In this case, a surface excess remains for the other components j . Once the position of the Gibbs surface is defined, the system is modeled as a bulk material with unaltered properties up to the dividing surface at which is added some excess quantity completely assigned to the Gibbs dividing surface (Figure 2.3b and Figure 2.5a). In this ideal scheme, the volume of the interfacial zone between the ideal bulk and the vacuum is zero (Figure 2.3a). Notice that elastic deformations change the position of the Gibbs surface [4].

3) It is sometimes called the Gibbs equimolar dividing surface.

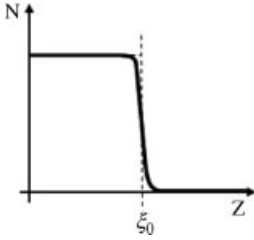


Figure 2.4 The location of the Gibbs dividing surface is chosen at the mathematical plane ξ_0 for which the surface excess number of a given specie vanishes ($N^{\text{surf}} = \int n(z)dz - N_A - N_B = 0$).

An alternative choice is to attach the dividing surface to a given piece of matter (Figure 2.5b) and, for instance, to treat the surface layers as a coating thin film with elastic properties different from those of the underlying bulk. The thickness of the film is thus arbitrary defined by the position of the dividing surface.

The two models must not be confused, even when the surface film is one monolayer thick. Indeed, these two idealized schemes (Figure 2.5a and b) correspond to different definitions of associated thermodynamics quantities. For instance, when using the ideal Gibbs dividing surface, the surface energy γ and the surface stress $s_{\alpha\beta}$ components are perfectly defined as excess quantities, which is not the case for the two-layer models (surface film plus bulk-like phase) for which the energy and the stress of the surface layer, respectively, are $E_{\text{layer}} = E_{\text{bulk}} + \gamma$ and $\tau_{\alpha\beta} = \sigma_{\alpha\beta} + s_{\alpha\beta}$, where E_{bulk} and $\sigma_{\alpha\beta}$, respectively, are the energy and the stress of a “bulk-like” monolayer.

For very thin films, the two surface zones shown in Figure 2.2 may overlap, making it impossible to define excess quantities with respect to the (nonexistent) bulk. Thus, the idealization of the dividing surface is valid only if the body is much larger than several atomic layers.

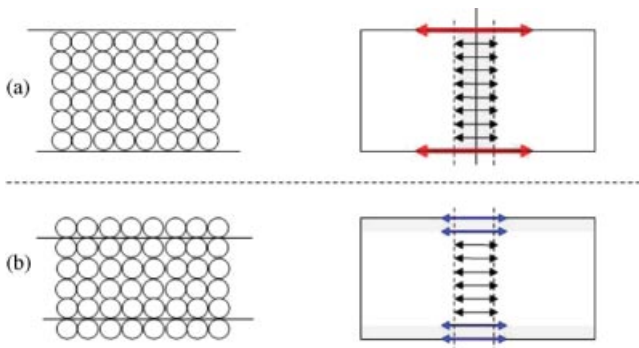


Figure 2.5 Two approaches to distinguish surfaces from the bulk. (a) Gibbs model in which surface excesses are ascribed to a mathematical plane (the dividing surface). (b) The surface can also be modeled as a thin film of thickness e . These models represent the variation in Figure 2.2.

2.2.3

Surfaces and Interfaces Described from Excess Quantities

Here, we will consider Gibbs' model (Figure 2.5a). For the sake of simplicity, we will write $x \equiv x_1$, $y \equiv x_2$, $z \equiv x_3$, with this last axis normal to the surface. Moreover, in what follows, Latin indices ($i, j = 1, 2, 3$) describe bulk properties, while Greek indices ($\alpha, \beta = 1, 2$) describe surface properties.

2.2.3.1 The Surface Elastic Energy as an Excess of the Bulk Elastic Energy

The elastic energy (Eq. (2.6)) is an extensive quantity that may be present in excess at the interface between two homogeneous materials as defined by Eq. (2.10). This excess quantity is defined as the difference between the elastic energy of the whole system and the sum of the elastic energies of the two homogeneous materials (see Figure 2.3):

$$\delta W^{\text{interf}} = \int_{z_A}^{z_B} \sum_{ij} \sigma_{ij}(z) \delta \varepsilon_{ij}(z) dV - \sum_{ij} \sigma_{ij}^A \delta \varepsilon_{ij}^A V^A - \sum_{ij} \sigma_{ij}^B \delta \varepsilon_{ij}^B V^B \quad (2.11)$$

where $\sigma_{ij}(z)$ and $\varepsilon_{ij}(z)$ are the bulk stress and strain profiles across the interface, while σ_{ij}^n and ε_{ij}^n (with $n = A, B$) are the homogeneous stress and strain tensors in the two homogeneous materials A and B separated by the interface (normal to the axis z). The interfacial quantity is the shaded area in Figure 2.3.

Equation (2.11) can be simplified when considering two physical conditions.

- i) The first condition is mechanical equilibrium that states that in absence of body forces, Eq. (2.4) gives (since there is only one variable $z = x_3$)

$$\frac{\partial \sigma_{i3}}{\partial x_3} = 0, \quad i = 1, 2, 3 \quad \forall x_3 \quad (2.12)$$

This means that the normal components of the stress tensor are homogeneous in the whole material:

$$\sigma_{iz}(z) = \sigma_{iz}^A = \sigma_{iz}^B \quad (2.13)$$

- ii) The second condition is a nongliding condition⁴⁾ that states that any infinitesimal change of the strain tensor components parallel to the interface must be the same in the whole material:

$$\delta \varepsilon_{\alpha\beta}(z) = \delta \varepsilon_{\alpha\beta}^A = \delta \varepsilon_{\alpha\beta}^B \quad (\alpha, \beta = 1, 2) \quad (2.14)$$

Using conditions (2.13) and (2.14), Eq. (2.11) becomes [5]

$$\delta W^{\text{interf}} / S^{AB} = \sum_{\alpha\beta} s_{\alpha\beta} \delta \varepsilon_{\alpha\beta} + \sum_i \sigma_{iz} \delta e_{iz} \quad (2.15)$$

4) Glissile epitaxy will be treated in Section 2.2.3.7.

where

$$s_{\alpha\beta} = \frac{1}{S^{AB}} \left[\int_{z_A}^{z_B} \sigma_{\alpha\beta}(z) dV - \sigma_{\alpha\beta}^A V^A - \sigma_{\alpha\beta}^B V^B \right] \quad (2.16)$$

and

$$e_{i3} = \frac{1}{S^{AB}} \left[\int_{z_A}^{z_B} e_{i3}(z) dV - e_{i3}^A V^A - e_{i3}^B V^B \right] \quad (2.17)$$

These equations suggest that we define the interfacial stress tensor

$$[s] = \begin{pmatrix} s_{11} & s_{12} & 0 \\ s_{21} & s_{22} & 0 \\ 0 & 0 & 0 \end{pmatrix} \quad (2.18)$$

and the interfacial strain tensor

$$[e] = \begin{pmatrix} 0 & 0 & e_{13} \\ 0 & 0 & e_{23} \\ e_{31} & e_{32} & e_{33} \end{pmatrix} \quad (2.19)$$

Notice that interfacial stress and interfacial strain are orthogonal tensors since $s_{ij}e_{ij} = 0$.

2.2.3.2 The Surface Stress and Surface Strain Concepts

Let us now consider the case where the phase B is vacuum so that $\sigma_{i3}^B = 0$ at mechanical equilibrium. In this case, Eq. (2.15) becomes

$$\delta W^{\text{surf}} = S^{AB} \sum_{\alpha\beta} s_{\alpha\beta} \delta \varepsilon_{\alpha\beta} \quad (2.20)$$

where

$$s_{\alpha\beta} = \frac{1}{S^A} \left[\int_{z_A}^{z_B} \sigma_{\alpha\beta}(z) dV - \sigma_{\alpha\beta}^A V^A \right] \quad (2.21)$$

now defines the surface stress as an excess quantity that generally is nonzero even if there is no stress in the bulk. Surface stress components may be positive (tensile) or negative (compressive).

Note that for a Hookean solid, the total elastic energy of a semi-infinite solid is the sum of a bulk elastic energy (Eq. (2.8)) and a surface elastic energy (Eq. (2.20)):

$$\delta W^{\text{el}} = \delta W^{\text{bulk}} + \delta W^{\text{surf}} = \frac{1}{2} \int_{i,j,k,l} C_{ijkl} \varepsilon_{ij} \varepsilon_{kl} dV + \int \sum_{\alpha\beta} s_{\alpha\beta} \varepsilon_{\alpha\beta} dS \quad (2.22)$$

For illustrative purposes, Figure 2.6 shows the calculated bulk energy versus normal deformation ε_{zz} (Figure 2.6a) and then versus in-plane deformation ε_{xx}

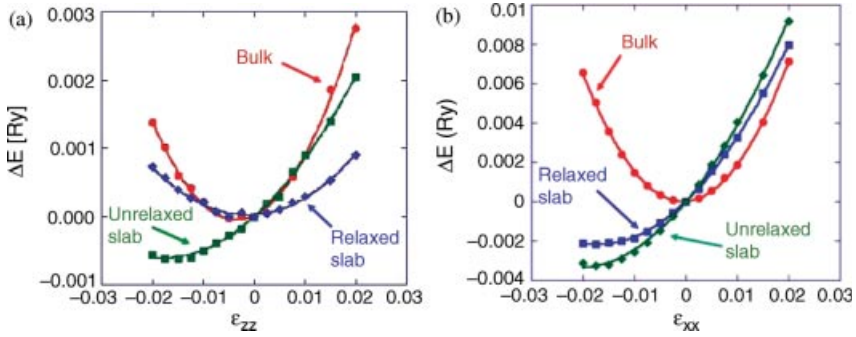


Figure 2.6 (a) Elastic energy versus strain ϵ_{zz} for a bulk material (circles), an unrelaxed slab (squares), and a relaxed slab (diamonds). (b) Elastic energy versus strain ϵ_{xx} for a bulk material (circles), an unrelaxed slab (squares), and a relaxed slab (diamonds). Note that when the elastic relaxation of the slab is properly taken into account, the parabola $\Delta E(\epsilon_{xx})$ is shifted but not the parabola $\Delta E(\epsilon_{zz})$. It means that the components $s_{iz} = 0$.

(Figure 2.6b). Three calculations have been performed: for a bulk material, for an unrelaxed slab of n layers, and for an elastically relaxed slab (*ab initio* calculations by Wien code [6], cubic material). For the slab, two calculations have been performed: the first one is for an unrelaxed slab and the second one for a relaxed slab.

Figure 2.6 shows that (i) for such small deformations, Hooke's law is valid (quadratic shape of the bulk energy); (ii) for unrelaxed slab, the surface stress shifts the parabola of the bulk energy that, according to (2.22), now contains a quadratic term and a linear term and roughly scales $C\epsilon^2 + s\epsilon$; and (iii) for an elastically relaxed slab, the bulk parabola is shifted for the in-plane deformation but remains centered on zero for the normal deformation. This last point (iii) simply illustrates that at mechanical equilibrium, surface stress components s_{iz} must be zero, so surface stress can be considered as a degenerated two-dimensional second rank tensor of order 2 (in the referential of the flat surface):

$$[s] = \begin{pmatrix} s_{11} & s_{12} \\ s_{21} & s_{22} \end{pmatrix} \quad (2.23)$$

Notice that Eq. (2.20) implies that the surface stress is the isothermal work per unit area against surface deformation at constant number of surface atoms. It must not be confused with the work done per unit area against surface creation at constant strain obtained by reversible cleavage, which is called surface energy (at least for pure materials). Figure 2.7 shows the main differences between surface stress and surface energy.

The surface energy γ is associated with breaking bonds. It can be calculated, at least at 0 K, by counting the broken bonds (and thus by adding interatomic potentials). The surface energy is a scalar quantity that scales as energy per unit area. The surface stress, which is a tensor, is associated with the work against surface deformation, and it is the result of forces acting at the material surface (and thus calculated as a sum of the first derivatives of the interatomic potentials). More precisely, if the surface is

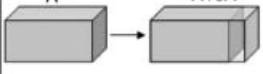
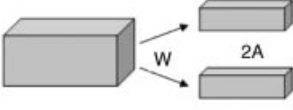
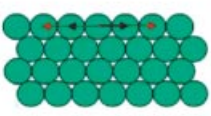
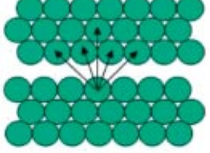
Surface stress	Surface energy
	
	
$dw_{et}^{surf} = \sum_{\alpha\beta} s_{\alpha\beta} d\varepsilon_{\alpha\beta}$	$\gamma = \frac{W}{2A} = \frac{1}{2A} [n_1\varphi_1 + n_2\varphi_2 + \dots]$

Figure 2.7 Difference between surface stress and surface energy. The surface stress originates from an elastic deformation and thus from bond stretching. It is an excess of stress at the surface (double arrows). Surface energy originates from

a cleaving process and thus from breaking bonds. It is thus calculated as the sum of bonds (A is the surface area and n_i the number of i th neighbors whose bonding energy φ_i are sketched by the arrows).

divided into parts by a curved boundary, where \vec{n} is the unit vector normal to the boundary in the surface plane, the surface stress tensor gives the force $f_i = \sum_j s_{ij} n_j$ exerted across the boundary curve.

2.2.3.3 Surface Elastic Constants

If a stress-free system is deformed in a direction parallel to the surface, a bulk stress will appear. For small deformations, Hooke's law is valid, so the total energy of a piece of the deformed matter (with surface and bulk contributions) is (up to the second order in strain)

$$E = E_0 + A_0\gamma_0 + A_0 \sum_{\alpha\beta} s_{0,\alpha\beta} \varepsilon_{\alpha\beta} + \frac{V_0}{2} \sum_{ijkl} C_{ijkl} \varepsilon_{ij} \varepsilon_{kl} \quad (2.24)$$

where E_0 is the cohesive energy, $A_0\gamma_0$ the surface energy, and the last term the elastic energy shared in its surface and bulk contributions (see Eqs (2.8) and (2.20)). (A_0 is the area of the free undeformed surface and $s_{0,\alpha\beta}$ the surface stress components.)

Equation (2.24) can be compared with the energy stored by an equivalent volume but without any surface:

$$E^{\text{bulk}} = E_0 + \frac{V_0}{2} \sum_{ijkl} C_{ijkl}^{\text{bulk}} \varepsilon_{ij} \varepsilon_{kl} \quad (2.25)$$

Comparing Eqs (2.24) and (2.25), we obtain

$$A_0\gamma_0 = [E - E^{\text{bulk}}]_{\varepsilon=0} \quad (2.26)$$

which defines the surface energy $\gamma_0 A_0$ as the surface excess of the cohesion energy measured at zero strain.

In the same way, we obtain

$$A_0 s_{0,\alpha\beta} = \left[\frac{\partial E}{\partial \varepsilon_{\alpha\beta}} - \frac{\partial E^{\text{bulk}}}{\partial \varepsilon_{\alpha\beta}} \right]_{\varepsilon=0} \quad (2.27)$$

which defines the surface stress as the surface excess of the first derivative of the cohesion energy versus bulk deformation.

Finally, the comparison of Eqs (2.24) and (2.25) gives

$$A_0 C_{ijkl}^{\text{surf}} = \left[\frac{\partial^2 E}{\partial \varepsilon_{ij} \partial \varepsilon_{kl}} - \frac{\partial^2 E^{\text{bulk}}}{\partial \varepsilon_{ij} \partial \varepsilon_{kl}} \right]_{\varepsilon=0} = V_0 \left[C_{ijkl} - C_{ijkl}^{\text{bulk}} \right] \quad (2.28)$$

which now defines the surface elastic constants C_{ijkl}^{surf} as the surface excess of the second derivative of the cohesion energy versus strain. The surface elastic constants measure how the surface stress changes with strain.

Note that

- i) From Eq. (2.28), the surface elastic constants can, in principle, be negative. It does not violate thermodynamic stability. Indeed, a surface cannot exist on its own, but must be supported by a bulk material. In other words, it is the total energy (surface plus volume) that ensures solid stability.
- ii) Since, at equilibrium, the components of the stress tensor perpendicular to the surface must be zero, every bulk elastic constants has not an excess at the surface. Table 2.1 lists the independent surface elastic constants for different plane point groups as reported by Shenoy [7]

$$s_{\alpha\beta} = s_{\alpha\beta}^0 + \sum_{\gamma\delta} S_{\alpha\beta\gamma\delta} \varepsilon_{\gamma\delta} \quad (2.29)$$

Table 2.1 Surface elastic constants.

Point group	Independent constants	Constraints
1, 2	All the 9 $S_{\alpha\beta\gamma\delta}$	No
1 m, 2 mm	$S_{1111}, S_{1122}, S_{1212}, S_{2211}, S_{2222}$	$S_{1112} = S_{1211} = S_{1222} = S_{2212} = 0$
4	$S_{1111}, S_{1112}, S_{1211}, S_{1212}, S_{1122}$	$S_{1122} = -S_{1211}, S_{2211} = S_{1122}$ $S_{2212} = -S_{1112}, S_{2222} = S_{1111}$
4 mm	$S_{1111}, S_{1122}, S_{1212}$	$S_{1112} = S_{1211} = S_{1222} = S_{2212} = 0$ $S_{2211} = S_{1122}, S_{2222} = S_{1111}$
3, 6	$S_{1111}, S_{1112}, S_{1122}$	$S_{1211} = -S_{1112}, 2S_{1212} = S_{1111} - S_{1122}$ $S_{1222} = S_{1112}, S_{2211} = S_{1122}$ $S_{2212} = -S_{1122}, S_{2222} = S_{1111}$
3 m, 6 mm	S_{1111}, S_{1122}	$S_{1112} = -S_{1211} = S_{1222} = S_{2212} = 0$ $2S_{1212} = S_{1111} - S_{1122}$ $S_{2211} = S_{1122}, S_{2222} = S_{1111}$

Adapted from Ref. [7].

Table 2.2 Relations between surface quantities.

	Euler	Lagrange
Excess energy	$A(\varepsilon)\gamma^E(\varepsilon) \approx A_0\gamma_0 + A_0s_0\varepsilon + \frac{A_0C_0^{\text{surf}}\varepsilon^2}{2}$	$A_0\gamma^L(\varepsilon) \approx A_0\gamma_0 + A_0s_0\varepsilon + \frac{A_0C_0^{\text{surf}}\varepsilon^2}{2}$
Surface energy	$\gamma^E(\varepsilon) \approx \gamma_0 + (s_0 - \gamma_0)\varepsilon + \frac{(C_0^{\text{surf}} - s_0)\varepsilon^2}{2}$	$\gamma^L(\varepsilon) \approx \gamma_0 + s_0\varepsilon + \frac{C_0^{\text{surf}}\varepsilon^2}{2}$
Surface stress	$s^E(\varepsilon) \approx \gamma_0 + \left. \frac{\partial \gamma^E}{\partial \varepsilon} \right _{\varepsilon=0} + (C_0^{\text{surf}} - s_0)\varepsilon$	$s^L(\varepsilon) \approx \left. \frac{\partial \gamma^L}{\partial \varepsilon} \right _{\varepsilon=0} + C_0^{\text{surf}}\varepsilon$

Adapted from Ref. [5].

meaning

$$S_{\alpha\beta\gamma\delta} = \frac{1}{S} \frac{\partial^2 W^{\text{surf}}}{\partial \varepsilon_{\alpha\beta} \partial \varepsilon_{\gamma\delta}} - s_{\alpha\beta}^0 \delta_{\gamma\delta}$$

in agreement with the simplified expression $s = s_0 + (C_0^{\text{surf}} - s_0)\varepsilon$, given in Table 2.2 for isotropic surface stress.

In Table 2.2 are shown the most useful relations valid for isotropic stresses and strains written in Eulerian (the reference state is the deformed state) and Lagrangian (the reference state is the undeformed state) coordinates.

2.2.3.4 Connecting Surface and Bulk Stresses

At mechanical equilibrium, the forces exerted by the surface to the underlying substrate must be equal and opposite to the distributed forces exerted by the bulk on the surface. It follows that the presence of surface stress results in nonclassical boundary conditions valid at equilibrium.

Mechanical equilibrium is achieved on much smaller timescales than shape equilibrium that needs mass transport. Mechanical equilibrium can thus be derived at constant surface shape. In other words, mechanical equilibrium is achieved when the first variation of W^{el} (given by (2.22)) with respect to a variation of displacement δu_i vanishes.

The first variation is

$$\delta W^{\text{el}} = - \int \sum_{ijkl} C_{ijkl} \frac{\partial \varepsilon_{kl}}{\partial x_j} \delta u_i dV + \int \sum_{i,j,k,l} C_{ijkl} \varepsilon_{kl} \delta u_i n_j dS + \int \sum_{\alpha\beta} s_{\alpha\beta} \varepsilon_{\alpha\beta} dS \quad (2.30)$$

Note that the last integral can be written as⁵⁾

$$- \int [\text{div}_S s + (s : \kappa) \vec{n}] \delta \vec{u} dS \quad (2.31)$$

5) For this purpose, it is enough to replace in (2.30) the strain components by the expressions of ε in terms of the derivative of the displacement field (see Eq. (2.1)) and then to use the divergence theorem.

where for the sake of readability, we avoid index notation and use the surface divergence operator div_S , the curvature tensor κ , and: for tensor product. Finally, \vec{n} is a unit vector normal to the surface.

Since at equilibrium the first variation δW^{el} must vanish for any arbitrary value of $\delta \vec{u}$, one obtains (with Eq. (2.7) and in absence of body forces) $f_i = \sum_j \partial \sigma_{ij} / \partial x_j = 0$ in the bulk and $\sigma_{ij} n_j = \text{div}_S s + (s : \kappa) \vec{n}$ at the surface or more precisely $\partial s_{\alpha\beta} / \partial x_\alpha = \sigma_{\alpha 3}$ and $\sigma_{ij} n_i n_j = s_{\alpha\beta} \kappa_{\alpha\beta}$. It is more convenient to project the last equations on the three-axis surface \vec{x}_i to get

$$\begin{cases} \sigma_{13} = \frac{\partial s_{11}}{\partial x_1} + \frac{\partial s_{12}}{\partial x_2} & \text{(a)} \\ \sigma_{23} = \frac{\partial s_{21}}{\partial x_1} + \frac{\partial s_{22}}{\partial x_2} & \text{(b)} \\ \sigma_{33} = \frac{s_{11}}{R_1} + \frac{s_{12}}{R_2} & \text{(c)} \end{cases} \quad (2.32)$$

where R_i are the principal curvatures.

Parts (a) and (b) in Equation (2.32) mean that, at the surface, the surface stress variation must be compensated by bulk shearing stresses. Moreover, note that the last equation is the Gibbs–Thomson equation, giving the Laplace overpressure in a curved crystal. Obviously, it reads $\sigma_{33} = 0$ for a free planar surface.

For completeness, Weissmüller and Cahn [8] have derived a general expression for the mean stress in microstructures due to interfacial stresses.

2.2.3.5 Surface Stress and Surface Tension

Using Eq. (2.15), the excess of internal energy at the free surface of a body becomes

$$dU^{\text{surf}} = T dS^{\text{surf}} + \sum_{\alpha\beta} s_{\alpha\beta} \delta \varepsilon_{\alpha\beta} A + \sum_i \mu_i dN_i^{\text{surf}} \quad (2.33)$$

where S^{surf} is the surface entropy, N_i^{surf} the number of particles in excess at the surface of chemical potential μ_i , and A the surface area [5].

Using the Euler integral of the surface excess energy [5] in the form $U^{\text{surf}} = TS^{\text{surf}} + \gamma A + \sum_i \mu_i N_i^{\text{surf}}$, we obtain the Gibbs–Duhem equation valid for a free surface [5]

$$d\gamma = - \frac{S^{\text{surf}}}{A} dT + \sum_{\alpha\beta} (s_{\alpha\beta} - \gamma \delta_{\alpha\beta}) \delta \varepsilon_{\alpha\beta} - \sum_n \Gamma_n d\mu_n \quad (2.34)$$

where Γ_n is the surface number density of particles n of chemical potential μ_n .

One of the derivatives of γ stemming from Eq. (2.34) gives the so-called Shuttleworth equation that connects surface stress and surface energy:

$$s_{\alpha\beta} = \gamma \delta_{\alpha\beta} + \left. \frac{\partial \gamma}{\partial \varepsilon_{\alpha\beta}} \right|_{\mu_n, T, \varepsilon_{iz}} \quad (2.35)$$

Equation (2.35) is obtained using the deformed surface (Eulerian coordinates) as a reference state. If the undeformed state is used (Lagrangian coordinates), the Shuttleworth relation becomes

$$s_{\alpha\beta} = \left. \frac{\partial\gamma}{\partial\varepsilon_{\alpha\beta}} \right|_{\mu_n, T, \varepsilon_{iz}} \quad (2.36)$$

Bottomley *et al.* [9] discuss the compatibility of the Shuttleworth equation with the Hermann formulation of thermodynamics. In response to Bottomley, subsequent works [10–13] clarified and validated the Shuttleworth relation.

2.2.3.6 Surface Stress and Adsorption

Another derivative of γ stemming from (2.34) gives the so-called Gibbs adsorption isotherm

$$\left. \frac{\partial\gamma}{\partial\mu_n} \right|_{T, \varepsilon_{ij}} = -\Gamma_n$$

which shows how the surface energy varies with respect to the chemical potential μ_n . Using this expression, the Shuttleworth Eq. (2.35) gives the surface stress change with respect to the chemical potential as

$$\left. \frac{\partial s_{\alpha\beta}}{\partial\mu_n} \right|_{T, \varepsilon_{ij}} = -\Gamma_n \delta_{\alpha\beta} - \frac{\partial\Gamma_n}{\partial\varepsilon_{\alpha\beta}} \quad (2.37)$$

For a Langmuir adsorption, the surface coverage θ linearly depends on the pressure P by means of

$$\frac{\theta}{1-\theta} = \frac{P}{P_\infty} \exp(\varphi/kT) \quad (2.38)$$

where P_∞ is a constant and φ the interaction energy between the adsorbate and its substrate.⁶⁾ In this case, using the Gibbs adsorption isotherm and Eq. (2.37), the surface stress and the surface energy change with coverage become [5]

$$\Delta\gamma = \frac{kT}{a^2} \ln(1-\theta) \quad \text{and} \quad \Delta s_{\alpha\beta} = \Delta\gamma \delta_{\alpha\beta} + \frac{\theta}{a^2} \frac{\partial\varphi}{\partial\varepsilon_{\alpha\beta}} \quad (2.39)$$

where $0 < \theta < 1$.

Some examples of the so-calculated surface stress change are shown in Figure 2.8a in case of Langmuir adsorption, where Eq. (2.39) is valid, and also in case of Bragg–Williams adsorption, where adsorbate–adsorbate interactions play a role (see Ref. [15]).

The surface stress change induced by an adsorbate can be measured. Consider a sheet (or a cantilever), a face of which is exposed to foreign molecules. Owing to the

6) Notice that $\Gamma_n = N_n/A$, where N_n is the number of adsorbed atoms and A the surface area, whereas $\theta n = N_n/N$, where N is the number of surface sites. At the same, the chemical potential is defined as $\mu = kT \ln(P/P_\infty)$.

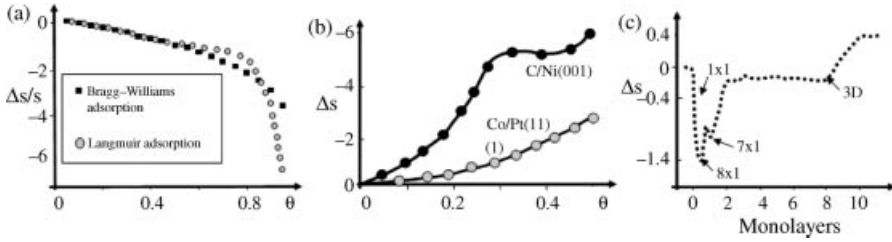


Figure 2.8 Surface stress versus adsorption: (a) Surface stress variation calculated for Langmuir adsorption and Bragg-Williams adsorption. Adapted from Ref. [15]. (b) Surface stress variation measured for C/Ni(1000) and Co/Pt(111). Adapted from Ref. [14]. (c) Surface stress variation versus coverage for Fe/W(001). Adapted from Ref. [18].

adsorption, the two sides of the sheet are no more in the same state of stress (see Eq. (2.39)), so the sheet spontaneously bends. The radius of curvature $R(\theta)$ is simply related to the surface stress difference by means of the Stoney formula [16] valid for thin isotropic sheets characterized by their Young modulus E and Poisson ratio ν :

$$\frac{1}{R(\theta)} = \frac{6(1-\nu)}{Eh^2} \Delta s(\theta) \quad (2.40)$$

Since the surface stress varies with the adsorbed coverage θ , the measurement of the coverage variation of the radius of curvature gives access to $s(\theta)$ when the surface stress of the bare sheet (before adsorption) is known. Note that for very thin films, the Stoney formula needs to be corrected [17].

Many experimental results on surface stress change with adsorption have been published (for a review, see Ref. [14]). For example, Figure 2.8b shows the surface stress change induced by carbon atoms adsorbed on Ni(001) surface. Figure 2.8b shows the surface stress change experimentally recorded for Fe/W(110) by Sander *et al.* [18]. In this last case, the sudden variations of surface stress versus coverage are associated with the appearance of successive surface phases. The case of nonhomogeneous adsorption has been studied by Bar *et al.* [19].

2.2.3.7 The Case of Glissile Interfaces

To be complete, notice that for glissile epitaxies, the description of stresses at the interface requires two interfacial tensors. One reflects the straining at constant deformation in both phases, while the other reflects the alteration of the interface structure at constant average strain [20, 21].

2.2.4

Surfaces and Interfaces Described as a Foreign Material

When using two-phase models (see Section 2.2.2), the surface is considered as a foreign thin film coating an underlying material. The basic equations consist of classical elastic equations valid for the bulk coupled to elastic equations valid for the film. Generally, the surface film cannot glide on the underlying bulk.

2.2.4.1 The Surface as a Thin Bulk-Like Film

In unorthodox approaches, the system (solid + surface) may be considered as a composite material constituted by two different materials.⁷⁾ As an illustration, let us consider the flexural rigidity (defined as the force torque required to bend a system to a unit curvature). For a single material, the flexural rigidity depends on the elastic modulus and the second moment of inertia of the sheet. For a multilayered composite, the flexural rigidity can be written as a function of the flexural rigidity of each of its layers. In a similar way, the flexural rigidity of a piece of body separated by a bulk core surrounded by a surface zone can be calculated by attributing specific elastic properties to the surface considered as a layer film with specific elastic constants and a given thickness. Notice again that this layered material (body + surface) simply is a pileup of bulk-like materials without any specific mechanical interfacial properties in the Gibbs meaning. Such models will be discussed in detail in Section 2.3.4.

2.2.4.2 The Surface as an Elastic Membrane

The main difference from the previous case is that now the film modeling the surface is considered to be an elastic membrane, that is, a material of negligible thickness and negligible flexural rigidity⁸⁾ bonded to a bulk substrate material. For the sake of simplicity, both materials (core + membrane) are generally assumed to be isotropic and described by two Lamé constants $\lambda^i = E^i \nu^i / ((1 - 2\nu^i)(1 + \nu^i))$ and $\mu^i = E^i / (2(1 + \nu^i))$, with $i = \text{surf}$ for the membrane and $i = \text{bulk}$ for the bulk material.

The stress tensor (of components τ_{ij}) characterizing the surface is defined by constitutive equations that ensure that the tractions transmitted by the membrane to the volume are equal and opposite to the force distribution in the bulk at which is added a displacement gradient which can be neglected when Lagrange and infinitesimal strains can be confused: [23–25]

$$\begin{cases} \tau_{\alpha\beta}^{\pm} = \tau^0 \delta_{\alpha\beta} + (\lambda^{\text{surf}} + \tau^0) \sum_k \varepsilon_{kk}^{\pm} \delta_{\alpha\beta} + (\mu^{\text{surf}} - \tau^0) \varepsilon_{\alpha\beta} + \tau^0 (\partial u_{\alpha}^{\pm} / \partial x_{\beta}) \\ \tau_{\alpha 3}^{\pm} = \tau^0 (\partial u_3^{\pm} / \partial x_{\alpha}) \end{cases} \quad (2.41)$$

where “±” refer to the up and down surfaces that, because of the deformation, cannot be in the same state of stress (Figure 2.9). In our context, the Lamé coefficients of the up and down surfaces are identical. The quantity τ^0 , called residual surface stress, under unconstrained conditions [23–25] may originate from thermal or mechanical treatment and thus is unrelated to s or γ .

The previous definition (Eq. (2.41)) of τ can be formally compared to the expression of s given in Eq. (2.29), meaning the sum of a stress in absence of deformation and a linear function of strain. Beyond the formal equivalence, let us note that the physical meaning of the various components of Eqs (2.29) and (2.41) are not the same since

- 7) One can thus distinguish three-phase model for plate (a core plus two opposite surfaces) from two-phase models valid for cylindrical or spherical objects (a core plus one surface).
- 8) Steigman and Ogden [22] took into account the flexural rigidity of the surface layers. In this case, there will be additional equilibrium equations, meaning that bending couples must vanish on the edge of the surface.

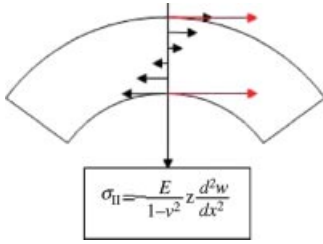


Figure 2.9 Sketch of the bulk stress variation (black arrows in the bulk) inside a curved sheet at which adds the surface stress (red arrows at the surface). *Inset:* Expression of the variation $\sigma_{xx}(z)$ versus the second derivative of the profile.

surface stress tensor $[s]$ is a true excess tensor (in the Gibbs meaning), but not $[\tau]$ except for some peculiar choice of the dividing surface.

2.3

Applications: Size Effects Due to the Surfaces

We will describe in turn how surface stress (i) induces spontaneous deformation of nanoparticles (Section 2.3.1), (ii) modifies the effective modulus of freestanding thin films (Section 2.3.2), and (iii) plays a role on the static bending of thin film (Section 2.3.3). At the same, we will consider the static bending of nanowires (Section 2.3.4).

Generally, we will use approaches expressed in terms of surface stress, but in some cases (according the state of the art) we will also use two-phase models.

2.3.1

Lattice Contraction of Nanoparticles

Following Ref. [26], let us take a free cubic crystal A with a rectangular shape of basis $\ell_x \ell_y$ and height ℓ_z . We will note s_A and s'_A , respectively, the surface stresses of the basal and lateral faces of the crystal. Let us now consider a virtual homogeneous deformation described by the bulk tensor ε_{ij} . The elastic energy due to this deformation is

$$W = W^{\text{bulk}} + W^{\text{surf}} \quad (2.42)$$

where, according to (2.6) and (2.20),

$$W^{\text{bulk}} = \frac{E \ell_1 \ell_2 \ell_3}{2((1+\nu)(1-2\nu))} [(1-\nu)(\varepsilon_{11}^2 + \varepsilon_{22}^2 + \varepsilon_{33}^2) + 2\nu(\varepsilon_{11}\varepsilon_{22} + \varepsilon_{11}\varepsilon_{33} + \varepsilon_{22}\varepsilon_{33})] \quad (2.43)$$

and

$$W^{\text{surf}} = 2s \ell_1 \ell_2 (\varepsilon_{11} + \varepsilon_{22}) + 2s'_A \ell_3 [\ell_1 (\varepsilon_{11} + \varepsilon_{22}) + \ell_2 (\varepsilon_{22} + \varepsilon_{33})] \quad (2.44)$$

The equilibrium strains are obtained by minimizing Eq. (2.42) with respect to strain. At equilibrium and for a square-shaped crystal $\ell_1 = \ell_2 \equiv \ell$, $\ell_3 = h$, we get

$$\varepsilon_{11}^{\text{eq}} = \varepsilon_{22}^{\text{eq}} = -\frac{1-\nu}{E} \left(\frac{2s_A}{h} + \frac{2s'_A}{\ell} \frac{1-3\nu}{1-\nu} \right), \quad \varepsilon_{33}^{\text{eq}} = -\frac{1-\nu}{E} \left(\frac{4s'_A}{\ell} - \frac{2s_A}{h} \frac{2\nu}{1-\nu} \right) \quad (2.45)$$

For a free cubic crystal, $h = \ell$ and $s_A = s'_A$, there is simply [26]

$$\varepsilon^{\text{eq}} = -4 \frac{1-2\nu}{E} \frac{s_A}{\ell} \quad (2.46)$$

A generalization of Eq. (2.46) valid for various shapes has been given in Ref. [27].

Injecting the equilibrium strain (2.46) into the total elastic energy (2.42) gives a negative value that for a freestanding cubic crystal reads $W = -6s_A \ell^2 \varepsilon^{\text{eq}}$. The negative sign means that due to its own surface stress, a small crystal is spontaneously deformed. Thus, it has a different crystallographic parameter compared to a large crystal (the deformation scales as ℓ^{-1}). If the surface stress is positive (respectively, negative), then the crystallographic parameter is smaller (respectively, greater) than the crystallographic parameter of the mother phase.

The measurement of such size-induced lattice contraction has been used to determine a mean value of the isotropic surface stress of cubic crystal [28–30]. More recent works [31] consider crystalline spheres (diameter D) cut in cubic crystals of compressibility K . In this case, (2.46) becomes $\varepsilon = -4Ks_A/3D$. In the absence of reliable values for surface stresses, the authors use asymptotic behaviors of surface energy combined with the Shuttleworth relation (2.35). In this way, the asymptotic form $s_A = [(3\gamma_0 a)/8K]^{1/2}$ (where a is an atomic unit and γ_0 the usual surface energy of the material) is more or less justified. The so-calculated deformations $\varepsilon = -(4K/3D)[(3\gamma_0 a)/8K]^{1/2}$ can be compared to experimental ones measured for various materials. The results are shown in Figure 2.10. Experiments and calculation clearly show the size effect. The deformations are negative, so the intrinsic surface

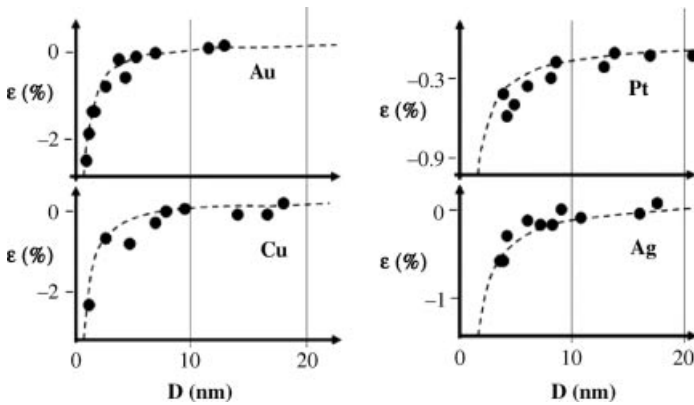


Figure 2.10 Lattice contraction (in %) of nanoparticles. Adapted from Ref. [31].

stress of these metals is positive and leads to a crystal contraction with respect to the mother phase. Notice that at the nanometer scale, deformations of a small percentage can be reached. Obviously, for such values, linear elasticity may become questionable. Let us stress again that two main assumptions have been used, isotropic surface stress and homogeneous deformation of the nanocrystal, so that only mean values of surface stress can be obtained by such methods.

2.3.2

Effective Modulus of Thin Freestanding Plane Films

Consider a nonsupported film ($\ell_2 = \ell_2 \rightarrow \infty$, $\ell_3 = h_0$) submitted to its own surface stress. The film is assumed not to bend. For the sake of simplicity, we will consider cubic crystals so that, at equilibrium, from (2.45)

$$\varepsilon_{11}^{\text{eq}} = \varepsilon_{22}^{\text{eq}} = \varepsilon = -\frac{2s_A}{h_0 Y} \quad \text{and} \quad \varepsilon_{33} = \frac{2\nu s_A}{E h_0} = -\frac{\nu}{1-\nu} \varepsilon \quad (2.47)$$

where $Y_0 = E/(1-\nu)$ is the usual elastic modulus defined as $Y_0 = (1/2)(d^2/d\varepsilon^2)$ (W^{Bulk}/V_0) in absence of any surface stress ($W^{\text{Bulk}} = Y_0 V_0 \varepsilon^2$ is the bulk elastic energy). In other words, (2.47) implies that because of its own surface stress, the film is, at equilibrium, deformed with respect to its bulk counterpart, so that the thickness of the film is no more h_0 but $h_0(1 + \varepsilon_{33})$ and the initial surface area A_0 becomes $A_0(1 + \varepsilon)^2$.

The total elastic energy per unit of nondeformed area (see Eq. (2.22)) of the system now becomes

$$\frac{W}{A_0} \approx Y_0 h_0 \varepsilon^2 + 4s_A \varepsilon \quad (2.48)$$

where the quadratic term due to bulk elasticity and the linear term due to surface stress again appear. The factor of 4 rises for the two in-plane directions and the two surfaces.

It is now possible to define an effective elastic modulus in presence of surface stress as $Y_{\text{eff}} = (1/2)(d^2/d\varepsilon^2)(W/V)$, where now $V = h_0 A_0 (1 + \varepsilon)^2 (1 + \varepsilon_{zz})$ is the volume after spontaneous deformation and W is given by (2.48). It is found that at mechanical equilibrium and up to the first order in $1/h_0$,

$$Y_{\text{eff}} \approx Y_0 + \frac{2s_A}{h_0} (2-\eta) \quad (2.49)$$

where $\eta = \nu/(1-\nu)$ scales as 1/2 for usual values of ν .

Equation (2.49) states that, due to surface stress, one can define an effective elastic modulus, the value of which varies as the reciprocal of the film thickness. Freestanding thin films with positive (respectively, negative) surface stress have a larger (respectively, lower) effective modulus than the material from which they have been cut.

This simple model has been extended and checked by Streitz *et al.* [32], who take into account higher order elastic effects by means of $Y_0(\varepsilon) = Y_0(1 - B\varepsilon)$ and

Table 2.3 Values determined from simulations of the (001) surfaces of various metals [32].

	Y_0 (eV/Å ³)	B	2η	s_A (eV/Å ²)	s_1 (eV/Å ²)	$2s_A \left[B + (4\eta - 3) + \frac{s_1}{s_A} \right]$
Cu	0.968	13.10	1.25	0.056	-0.14	1.13
Ni	1.542	14.70	1.08	0.047	0.07	1.44
Ag	0.623	13.73	1.36	0.050	-0.19	0.97
Au	0.628	14.61	1.58	0.077	-0.38	1.51

$s_A(\varepsilon) = s_A + s_1\varepsilon$, so the total elastic energy now becomes

$$\frac{W}{A_0} \approx 4s_A\varepsilon + (Y_0h_0 + 2s_A + 2s_1)\varepsilon^2 + \frac{2}{3} \left[Y_0h_0 \left(3 - \frac{3}{2}\eta - \frac{B}{2} \right) + 2s_1 \right] \varepsilon^3 \quad (2.50)$$

Equation (2.49) then up to the first order in $1/h_0$ becomes

$$Y_{\text{eff}} \approx Y_0 + \frac{2s_A}{h_0} \left[B + (4\eta - 3) + \frac{s_1}{s_A} \right] \quad (2.51)$$

While in the linear approximation the elastic nature of the freestanding film (softer or stiffer than that of its bulk counterpart) depends only on the sign of the surface stress of the body (see Eq. (2.49)), it is no longer the case when nonlinear effects are taken into account (see Eq. (2.51)). More generally (for more complex shapes), it can be shown that the effective Young modulus depends on the third-order bulk and elastic constants [27].

Streitz *et al.* [32] used (2.51)⁹ to calculate the equilibrium strain and the effective modulus for various metals for which they calculate surface stress s_A , the usual Young modulus Y_0 , and the higher order elastic constants B and s_1 . The results of their calculations are shown in Table 2.3. It appears that B is positive, scales as s_1/s_A , and is greater than unity. It follows that the leading term in Eq. (2.51) is not the surface stress by its own, but it is the coupling between the higher order constants (s_1 and B) and the surface stress s_A by means of $\Delta Y \approx 2s_A B/h_0$. The strain (calculated from the formula given in footnote 9) and the effective modulus (calculated from Eq. (2.51)) with the data given in Table 2.3 are shown in Figure 2.11, in which the same quantities calculated by molecular dynamics simulations are also shown [32]. There is an excellent agreement but notice that the sizes at which the surface effect cannot be negligible are at the nanoscale.

As a conclusion, the elastic modulus of a freestanding thin film is actually determined by nonlinear elastic properties of its bulk and surface (for a complete discussion, see Ref. [33]).

9) Note that the equilibrium strain is not given by Eq. (2.47), but by $\varepsilon^{\text{eq}} \approx -2s_A/(4h_0 + 2s_1 + h_0 Y_0)$. Moreover, note that (2.49) cannot be recovered by simply putting $B = 0$ and $s_1 = 0$ in (2.51) because both expressions are not at the same order in strain.

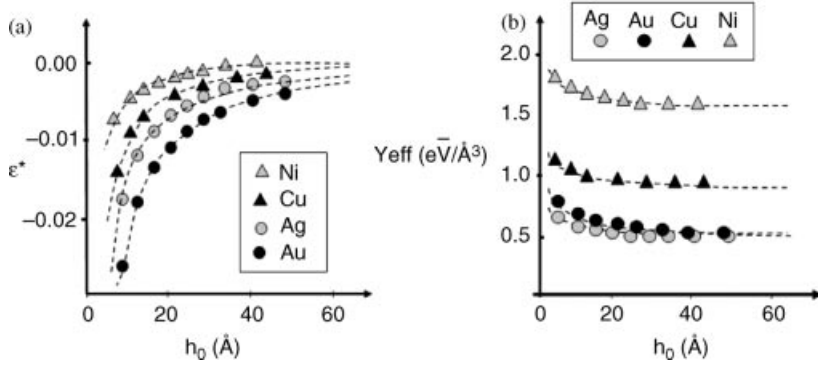


Figure 2.11 (a) Strain versus thickness calculated for various metals. Adapted from Ref. [32]. (b) Corresponding effective modulus. Adapted from Ref. [32].

2.3.3

Bending, Buckling, and Free Vibrations of Thin Films

2.3.3.1 General Equations

We will now consider bending, buckling, and free vibrations of thin films when incorporating surface elasticity effects. The main formulation consists of adding surface forces and bending moments due to surface stress to the equations of the classical description of a plate. Indeed, let us consider a thin asymmetric, isotropic sheet of thickness e . The faces 1 and 2, respectively, bear surface stress $s_{\alpha\beta}^1$ and $s_{\alpha\beta}^2$. These surface stresses generate two moments, a first moment (a force) and a second moment (a torque).

The first moment is $N_{\alpha\beta}^{\text{surf}} = \int_{-e/2}^{e/2} [s_{\alpha\beta}^1 \delta(x_3 + e/2) + s_{\alpha\beta}^2 \delta(x_3 - e/2)] dx_3$, so using the sifting properties of the Dirac function $\delta(x)$, we get

$$N_{\alpha\beta}^{\text{surf}} = s_{\alpha\beta}^1 + s_{\alpha\beta}^2 = \Delta s_{\alpha\beta}^+ \quad (2.52)$$

This moment, which depends on the total surface stress $\Delta s_{\alpha\beta}^+$, is equivalent to a resultant force per unit length applied on the medium plane. This results in the strength of the medium plane.

The second moment $M_{\alpha\beta}^{\text{surf}} = \int_{-e/2}^{e/2} [s_{\alpha\beta}^1 \delta(x_3 + e/2) + s_{\alpha\beta}^2 \delta(x_3 - e/2)] x_3 dx_3$ can also be calculated:

$$M_{\alpha\beta}^{\text{surf}} = (s_{\alpha\beta}^1 - s_{\alpha\beta}^2) e/2 = \Delta s_{\alpha\beta}^- e/2 \quad (2.53)$$

which depends on the differential surface stress $\Delta s_{\alpha\beta}^-$. This moment is a torque that bends the sheet (Figure 2.12). Let us recall that because of the bending, the stresses are not constant in the bulk but vary with the altitude (see Figure 2.9).

The total moments in the presence of bulk stress and surface stresses are the sum of the bulk and surface moments and can be written as

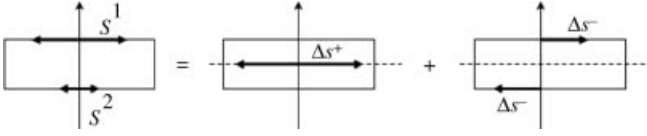


Figure 2.12 Sketch of the decomposition of the differential of surface strain in the first moment applied in the medium plane and a second moment that is a couple that tends to bend the sheet.

$$N_{ij}^{\text{tot}} = N_{ij} + N_{\alpha\beta}^{\text{surf}} = \int_{-e/2}^{e/2} \sigma_{ij} dx_3 + \Delta s_{\alpha\beta}^+, \quad M_{ij}^{\text{tot}} = M_{ij} + M_{\alpha\beta}^{\text{surf}} = \int_{-e/2}^{e/2} \sigma_{ij} x_3 dx_3 + \Delta s_{\alpha\beta}^- e/2 \quad (2.54)$$

The equations of motion for the body (see Eq. (2.3)) of the plate are

$$\frac{\partial \sigma_{ij}}{\partial x_j} + f_i = \rho \frac{d^2 u_i}{dt^2} \quad (2.55)$$

Equation (2.55) accounts for the body forces (e.g., gravity, see footnote 2) of components f_i . Again, ρ is the density and u_i the components of the displacement field.

Equation (2.55) can be multiplied by dx_3 or $x_3 dx_3$ and then integrated to get the equations of motion governing the resultant moments [34, 35].

$$\frac{\partial N_{i\alpha}}{\partial x_\alpha} + \sigma_{i3}^{\text{up}} - \sigma_{i3}^{\text{down}} + \int_{-e/2}^{e/2} f_i dx_3 = \int_{-e/2}^{e/2} \rho \frac{d^2 u_i}{dt^2} dx_3 \quad (2.56)$$

$$\frac{\partial M_{i\beta}}{\partial x_\beta} - N_{i3} + \frac{e}{2} (\sigma_{i3}^{\text{up}} + \sigma_{i3}^{\text{down}}) + \int_{-e/2}^{e/2} f_i x_3 dx_3 = \int_{-e/2}^{e/2} \rho \frac{d^2 u_i}{dt^2} x_3 dx_3 \quad (2.57)$$

where σ_{i3}^{up} and $\sigma_{i3}^{\text{down}}$ are the stress at the up and down surfaces, respectively.

The mechanical equation valid for the upper and lower surfaces (respectively, labeled (+) and (-)) reads

$$\frac{\partial s_{\beta i}^\pm}{\partial x_\beta} - \sigma_{i3}^\pm = \rho \ddot{u}_i^\pm$$

where we write $d^2 u/dt^2 = \ddot{u}$. Obviously, at equilibrium this latter equation is Eq. (2.32).

The previous mechanical equation can be inserted into Eqs (2.56) and (2.57) to obtain

$$\frac{\partial}{\partial x_\alpha} (N_{i\alpha} + \Delta s_{\beta i}^+) + \int_{-e/2}^{e/2} f_i dx_3 = \int_{-e/2}^{e/2} \rho \cdot \ddot{u}_i dx_3 + \rho (\ddot{u}_i^1 + \ddot{u}_i^2) \quad (2.58)$$

$$\frac{\partial}{\partial x_\beta} \left(M_{\alpha\beta} + \frac{e}{2} \Delta s_{\alpha i}^- \right) - N_{\alpha 3} + \int_{-e/2}^{e/2} f_i x_3 dx_3 = \int_{-e/2}^{e/2} \rho \cdot \ddot{u}_\alpha x_3 dx_3 + \frac{e}{2} \rho (\ddot{u}_\alpha^1 - \ddot{u}_\alpha^2) \quad (2.59)$$

At equilibrium (no time dependence) and in absence of body forces, these equations become

$$\frac{\partial}{\partial x_\alpha} (N_{i\alpha} + \Delta s_{\beta i}^+) = 0 \quad (2.60)$$

$$\frac{\partial}{\partial x_\beta} \left(M_{\alpha\beta} + \frac{e}{2} \Delta s_{\alpha i}^- \right) = N_{\alpha 3} \quad (2.61)$$

These equilibrium equations have to be solved with well-defined boundary conditions.

2.3.3.2 Discussion

Most of the surface stress-induced modifications of the usual behavior of thin plates [34–41] have been studied with a surface modeled as a foreign membrane [23–25]. However, owing to the analogy between Eqs (2.29) and (2.39), the results are comparable to those obtained with the true surface stress in the Gibbs meaning.

Usually two assumptions can be found in the literature. The first, the thin film assumption, is that σ_{33} is zero inside the whole film.¹⁰⁾ The second assumption is a linear variation of σ_{33} in the film as, for instance, $\sigma_{33} = (1/2)(\sigma_{33}^+ + \sigma_{33}^-) + (1/h)(\sigma_{33}^+ - \sigma_{33}^-)x_3$. Here, we will illustrate only surface effects in the framework of the thin film approximation and Kirchhoff theory¹¹⁾ [34–38]. For this purpose, consider an isotropic material (bulk and surfaces) in which an infinitely long (in the x_2 direction) sheet of finite width ℓ in direction x_1 and thickness e is cut. The (dimensionless) results of Ref. [38] are shown in Figure 2.13 for the maximum deflection, the load at which the sheet buckles, and the frequency of vibration. The materials constants are $E = 5.625 \times 10^{10}$ N/m², $\nu = 0.25$, $\rho = 3 \times 10^3$ kg/m³, $\lambda_0 = 7 \times 10^3$ N/m, $\mu_0 = 8 \times 10^3$ N/m (the Lamé coefficients of surfaces), and the residual surface stress $\tau_0 = 110$ N/m (more details can be found in Ref. [35]). It is easy to see in Figure 2.13 that the static as well as the dynamic response of a sheet depends on its surface properties. Obviously, the thinner the sheet, the proportionally greater the surface effects. Notice that the surface may help or oppose the external stress according to the sign of the stress $[\tau]$ (given by Eq. (2.41)) at the surface. For the thinner sheets, surface stress effects can become so important that nonlinear

¹⁰⁾ At mechanical equilibrium, σ_{33} must vanish at the free surfaces.

¹¹⁾ In the classical thin plate description, two theories can be encountered: the Kirchhoff plate theory and the Mindlin plate theory that differs only by the assumptions on the asymptotic form of the displacement fields.

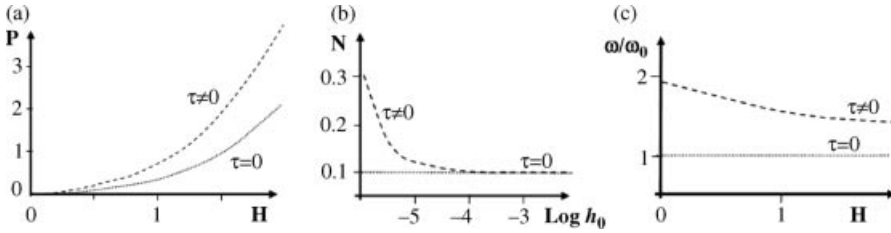


Figure 2.13 Surface effect on bending, buckling, and free vibration of a sheet with edges at $x_1 = 0$ and $x_1 = \ell$ and $\tau_0 = 110 \text{ N/m}$ and $h_0 = 10^{-6} \text{ m}$. Adapted from Ref. [35].
 (a) $P = 100(1-\nu^2)P_0E$ versus H for a simply supported sheet. $P = P_0 \sin(\pi x_1/\ell)$ is the transverse load and H the reduced sag (w/h_0).
 (b) $N = 12(1-\nu^2)T/Eh$ versus $\text{Log } h_0$ (h_0 in meter) for a simply supported sheet at both

edges submitted to a pair of compressive forces of amplitude T . A strong negative surface stress may the sheet buckled without any external stress. (c) Reduced frequency of vibration versus the reduced sag (w/h_0) for a simply supported sheet submitted to vertical displacement, $u_3 = U \sin(\pi x_1/\ell)$. Notice that $\tau = 0$ means no surface effects ($\tau_0, \lambda_0, \mu_0 = 0$).

elasticity effects may play a role. However, the result is that the size-dependent behavior originates from the strain dependence of the surface stress, that is, from the surface elastic constants. In other words, the usual results of the thin plate are recovered for zero or constant surface stress. It is only when surface elastic constants are introduced that there can be a stiffening or a softening of the material, as more recently confirmed by the analytical calculations of Refs [42, 43]. Again, the surface effect is significant for film thinner than 10 nm.

A simple proof of this conclusion is given in Ref. [44]. The energy of vibration (per unit length) of a rectangular beam (length L , height $2h$, width ℓ) prestressed by its surface stress can be written as the sum of its bulk and surface energies [1, 44] (s is the surface stress assumed to be isotropic):

$$W = \frac{1}{2} \int_0^L (EIy''^2 - Fy'^2) dx + \int_0^L \ell s y'^2 dx \quad (2.62)$$

where E is the bulk Young modulus, I the moment of inertia, F a bulk compressive force that prestress the sample and, at equilibrium, balance the forces exerted by the surfaces, and $y(x, t)$ the vertical deflexion (the primes denote the derivatives with respect to x). Since the equilibrium requires $F = 2s\ell$, the total energy (2.62) is independent of surface stress.

When taking into account surface elasticity by means of $s = s_0 + S^{\text{surf}} \varepsilon$, where S^{surf} is a surface elastic constant and $\varepsilon \approx hy''$ the strain at the surfaces, a term $\int_0^L \ell S^{\text{surf}} \varepsilon^2 dx$ adds to (2.62), so

$$W = \frac{1}{2} \int_0^L (EI + 2S^{\text{surf}} \ell h^2) y''^2 dx \quad (2.63)$$

We can define an effective modulus

$$E_{\text{eff}} = E + \frac{2S^{\text{surf}} \ell h^2}{I} \quad (2.64)$$

which depends on the shape (via I) and the surface elasticity (via S^{surf}). The frequency of vibration of the cantilever $\omega^2 = \omega_0^2(1 + (2S^{\text{surf}} \ell h^2 / EI))$ [44] does not depend on s , but only on the strain dependence of the surface stress, that is, on surface elasticity.¹²⁾ Notice that more recently finite element method calculations have confirmed this result [45].

2.3.4

Static Bending of Nanowires: An Analysis of the Recent Literature

Static and dynamic bending tests have been widely reported for nanowires [46–49]. The experiments are complex. In particular, it is generally hard to control the boundary conditions, so there is a wide scattering in the experimental data (see Section 2.3.5). However, most of the experiments show that the elastic behavior of a nanowire is different from the elastic behavior of its bulk counterpart (or mother phase), affecting the size-dependent modulus that can be softer or harder than the modulus of the bulk material. Again, this size effect essentially comes from the surface/bulk ratio.

Notice that for rectangular wires, the presence of two pairs of free surfaces gives additional effects due to edges and corners. In the following section, we will study only the simpler case of cylindrical wires.

2.3.4.1 Young Modulus versus Size: Two-Phase Model

For nanowires, most previous works use a two-phase model in which the wire is divided in a cylindrical core of radius r_0 surrounded by a shell of thickness e , so that the diameter of the whole wire is $D = 2(r_0 + e)$. The core and the shell are, respectively, characterized by their elastic modulus E_0 and E_s . The flexural rigidity of the nanowire is written as $EI = E_0 I_0 + E_s I_s$, where I_0 and I_s are the moment of inertia of cross section of the core and the sheet.

Using the expression of the inertia momentum, the effective modulus of the wire is [48]

$$E = E_0 \left[1 + 8 \left(\frac{E_s}{E_0} - 1 \right) (\eta - 3\eta^2 + 4\eta^3 - 2\eta^4) \right]$$

where $\eta = e/D$.

A fit of the experimental data gives the surface thickness e and the ratio E_s/E_0 . However, this phenomenological ratio cannot be simply interpreted in terms of elastic constants.

¹²⁾ Some authors omit F and thus find that E_{eff} depends on s , which is clearly wrong [44].

He and Lilley [40] have extended this approach to different boundary conditions and different geometries (rectangular or circular cross section). However, their approach is slightly different since they introduce an additional distributed transverse force due the stress jump across the surface $\Delta\sigma_{ij}n_i n_j = s_{\alpha\beta}K_{\alpha\beta}$ (n_i are the components of the unit vector normal to the surface and $K_{\alpha\beta}$ the curvature tensor so that $s_{\alpha\beta}K_{\alpha\beta}$ simply is the Laplace overstress) written as $s_0\gamma''(x)$ for an isotropic surface stress ($\gamma(x)$ is the transverse displacement). The equilibrium equation $EI\gamma''''(x) = 2Ds_0\gamma''(x)$ is thus solved for different boundary conditions: a cantilever (submitted to a concentrated load force at its end), a simply supported wire, and a clamped wire (submitted to a concentrated load force applied to the middle of the wire). The main result is that a positive surface stress s_0 opposes concave curvature of the mean plane of the wire and enhances convex curvatures. For positive surface stress, the cantilever behaves as a softer material, while a simply supported or clamped sheet behaves as a stiffer material (compared to its bulk counterpart). This result could illustrate why quantifying the mechanical properties at the nanoscale is so challenging. Indeed, the effective modulus appears to depend on the boundary conditions! However, as shown in Section 2.3.3.2 and Ref. [44], this analysis neglects the prestress effect the surface stress (considered as a membrane) induces, so the true equilibrium equation should be $EI\gamma''''(x) = -F\gamma''(x) + 2Ds_0\gamma''(x)$, where at equilibrium the compressive axial force due to surface stress is $F = 2D\ell s_0$. This prestress effect thus should modify the surface stress effect in the absence of surface elasticity (see Section 2.3.4.3).

2.3.4.2 Young Modulus versus Size: Surface Stress Model

Cuenot *et al.* [46] have reported effective modulus measured for ZnO nanowires: the smaller the diameter of a nanowire, the greater its effective modulus. To interpret these experimental results, the total bending energy due to a force F applied on the wire inducing a deflection δ is [46] $U = -F\delta + (1/2)k\delta^2 + \pi D\Delta L(1-\nu)$, where the first term is the work of the applied force F , the second term the bulk elastic energy depending on the stiffness modulus k of the bulk material of the wire, the last term the work against surface deformation, where s is the surface stress (assumed to be isotropic), and $\Delta L = (12/5)(\delta^2/L)$ the extension of the wire. For clamped wires, the total energy becomes $U = -F\delta + (1/2)k_{\text{eff}}\delta^2$, where $k_{\text{eff}} = k + (24/5)s(\pi D/L)(1-\nu)$. For the geometry of the wire, $E = (L^3/192I)k$, where $I = \pi D^4/64$ is the moment of inertia of the section, so Cuenot *et al.* [46] define an effective modulus $E_{\text{eff}} = E + (8/5)s(1-\nu)(L^2/D^3)$. Again, even if experimental data are well fitted by the model, the model neglects the prestress bulk induced by the surface stress (see footnote 12).

2.3.4.3 Prestress Bulk Due to Surface Stresses

We have seen that most of the recent works neglect the bulk stress initially induced by the surface stresses. The effect of this prestress has been properly taken into consideration by Wang *et al.* [50] in the case of pure bending of nanowires. For this purpose, they consider an isotropic nanowire of thickness h , width b , and length ℓ and isotropic surface stress s . The authors (i) calculate the bulk stress (supposed to be

homogeneous) due to the surface stress (as in Section 2.3.1), (ii) calculate the strain field in the bulk and at the surface, the (iii) the strain-dependent surface stress, and (iv) the bulk and surface elastic energies. Let us underline that the authors allow the nanowire to relax axially at its ends. They can thus define an effective Young's modulus that can be expressed as

$$E_{\text{eff}} = E + E_{\text{surf}} \left(\frac{6}{h} + \frac{2}{b} \right) + 2 \frac{s}{h} \left(2\nu^2 \left(\frac{b}{h} \right)^2 - \left(\frac{\ell}{h} \right)^2 \right) \quad (2.65)$$

where E_{surf} , a surface Young's modulus, is a combination of the surface elastic constants.

This equation can be formally compared to Eqs (2.49) and (2.51) obtained for thin freestanding planar films (that are not allowed to bend) or to Eq. (2.64) obtained from vibration properties.

The main conclusion is that Young's modulus can be considerably affected by the surface properties. It is modified not only by the absolute size of the nanowire but also by its aspect ratio. More precisely, for positive elastic constants and positive surface stress, the effective Young's modulus decreases with the decrease in the nanowire thickness or the increase in its aspect ratio. Let us underline that this result has been obtained for free boundary conditions. It could be different for clamped conditions (see the discussion in Section 2.3.5). Again, Eq. (2.65) predicts that stress effects play a role only at the nanoscale (roughly for thickness smaller than 20 nm) [50].

2.3.5

A Short Overview of Experimental Difficulties

We cannot end this short review of surface effects on elastic properties of nanoscale objects without any analysis of the experimental uncertainties that concern the sample preparation, the sample characterization, the mechanical system used to excite the nano-object, and even the simple definition of the object geometry. We list below some of the experimental difficulties.

Most of the methods used to fabricate micro- or nanoscale objects employed techniques that potentially affect the mechanical behavior by ions implantation, surface amorphization, surface roughness, or even dislocation implantation [51].

The mechanical probe is generally larger than the size of the object [47–60], so the mechanical properties of the whole system (probe + object) should be checked. Furthermore, the boundary conditions (clamping, simply supported, free boundary) are difficult to define accurately and to reproduce from one experiment to another. It is all the more important that, as numerically shown by Park and Klein [61], effective Young's modulus depends on the boundary conditions. For instance, they [61] found (for gold) that increasing the nanowire aspect ratio leads to an increase (respectively, decrease) in E_{eff} for clamped (respectively, free ended) nanowire. This can be easily understood since the clamped condition prevents the axial relaxation due to surface stress. The experimental difficulties due to the boundary conditions can be

partially overpassed by using acoustic methods that simply excite the vibrational modes [62, 63] without contact.

It is sometimes difficult to accurately characterize the geometry of a nano-object (for instance, the diameter of a nanowire is not necessarily constant on its whole length). An error of 5% on the nanowire scales leads to an uncertainty of 25% on the effective Young modulus.

Since plastic properties are also size dependent [52, 53], the knowledge of the dislocation density may be crucial. Indeed, the mechanical properties cannot be the same if the object already contains a dislocation that can move under the external force or if it is necessary to create the dislocation before activating it.

All these limitations may be at the origin of the large dispersion of the available experimental results and even at the origin of several systematic errors. For instance, most of the theoretical calculations predict size effects at the nanometer scale, while a few experiments show size effects that already occur at some hundred of nanometers! May be some of these experimental results have not been obtained with a well-defined system. For instance, the Young modulus of a vibrating cantilever has been found to decrease [56], increase [64], or to be constant [60] according to the cantilever diameter,¹³⁾ while Raman scattering of nanoparticles does not put in evidence any size dependence of the Young modulus [62, 63]. The analysis of the mechanical properties of cantilevers with varying width seems to be a necessary challenge [65].

2.4

Conclusion

A great deal of research has been done on the elastic properties of nanoscale materials. Like many other properties, the mechanical properties of small objects deviate from those of macroscopic objects of the same material. The overall elastic behavior of nanosized objects is size dependent. This size dependence originates from proportionally greater surface effects. Indeed, the surface has bond length and strength different from the volume, so a nanoscale object must, at least, be divided into a bulk core and a surface zone with different properties. The surface zone can be described in various ways. The best one consists of using the concepts of dividing surface and surface excess. The main advantage is that the so-defined quantities are perfectly defined from a thermodynamic viewpoint. Other choices are possible, but in all the cases the localization of the dividing surface should be specified before any calculation. In some cases, it is easier to split the dividing surface into two surfaces separated by a distance that defines the surface thickness. When specific elastic properties are attributed to surfaces, the elastic behavior of a finite-size body results from a subtle interplay between its bulk and surface properties and thus depends on the absolute size of the object. Such size dependence becomes significant when at least one dimension becomes smaller than, let us say, a few tens of nanometers.

13) But obviously the effect depends on the sign and the value of the surface stress of the material.

Most of the mechanical characteristics of nanoscale objects can be inferred from models coming from surface physics in which the surface is characterized by an excess of stress in the Gibbs meaning. More precisely, it is possible to show with these models that because of surface stress, the crystallographic parameter, the Young modulus, the flexure rigidity, and so on of nanoscale structures differ from those of bulk (infinite) materials. However, surface stress alone is not enough to explain all the experimental occurrences. In particular, surface elastic constants have to be introduced since the stiffening effect is essentially due to the strain dependence of the surface stress. Moreover, at the nanoscale surface stress may induce huge bulk strain, so the whole mechanical behavior can no more be described by linear elasticity theory. In some cases, the surface stress effect, by its own, is less important than the nonlinear behavior it induces in the bulk [66]!

Finally, notice that since surface effects are dominant at the nanoscale, the elastic properties also depend on the shape of the objects. It is clearly put in evidence in Ref. [27] in the case of Cu. For nanowires, the Young modulus increases as the wire becomes thinner, while for a freestanding film, it decreases.

Again, let us underline that mechanical tests at the nanoscale are still a challenge. In particular, since most of the tools used for the stress measurements are at the macroscale, it is generally hard to control the boundary conditions. At the same, it is difficult to simply control the initial state (surface roughness, defects density, and even geometrical data as initial curvature or size) with a good accuracy. It results in a wide scattering in the experimental data, so efforts have to be made to access better data even if some statistical attempts to go round these intrinsic limitations have been explored [67].

From a theoretical viewpoint, let us notice again that the models coming from surface physics cannot be applied to the smallest sizes at which it is no more possible to divide the piece of matter into a core and a surface zone. In this case, it is necessary to resort to atomistic approaches expressed in terms of spring models, pseudopotentials, or *ab initio* calculations [66, 68] or may be to use nonlocal elasticity [69]. Moreover, let us notice that strained nanowires may be morphologically unstable. Such instabilities are beyond our scope of this book, but the reader can refer to Refs [70–72].

Acknowledgment

I wish to acknowledge Ezra Bussmann, Raymond Kern, and Andres Saul for fruitful discussions.

References

- 1 Landau, L. and Lifshitz, E. (1970) *Theory of Elasticity*, Pergamon Press, Oxford.
- 2 Timoshenko, S. and Goodier, J. (1951) *Theory of Elasticity*, McGraw Hill, New York.

- 3 Gibbs, J.W. (1928) *The Collected Works of J.W. Gibbs*, Longmans, Green and Company, New York, p. 1928.
- 4 Nozieres, P. and Wolf, D.E. (1988) Interfacial properties of elastically strained materials. *Z. Phys. B*, **70**, 507–512.
- 5 Müller, P. and Saül, A. (2004) Elastic effects on surface physics. *Surf. Sci. Rep.*, **54**, 157–258.
- 6 Saül, A. and Müller, P. (2011) in preparation.
- 7 Shenoy, V. (2005) Atomistic calculations of elastic properties of metallic fcc crystal surfaces. *Phys. Rev. B*, **71**, 094104.
- 8 Weissmüller, J. and Cahn, W. (1997) Mean stresses in microstructures due to interface stresses: a generalization of a capillary equation for solids. *Acta Mater.*, **45**, 1899–1906.
- 9 Bottomley, D.J. (2009) Incompatibility of the Shuttleworth equation with Hermann's mathematical structure of thermodynamics. *Surf. Sci.*, **603**, 97–101.
- 10 Ibach, H. (2009) Comments on the article entitled "Incompatibility of the Shuttleworth equation with Hermann's mathematical structure of thermodynamics". *Surf. Sci.*, **603**, 2352.
- 11 Marichev, V. (2008) Comment on "Incompatibility of the Shuttleworth equation with Hermann's mathematical structure of thermodynamics". *Surf. Sci.*, **602**, 1131.
- 12 Erickson, J. and Rusanov, A. (2009) Comments on "Incompatibility of the Shuttleworth equation with Hermann's mathematical structure of thermodynamics". *Surf. Sci.*, **603**, 2348.
- 13 Hecquet, P. (2010) Comments on the article entitled "Incompatibility of the Shuttleworth equation with Hermann's mathematical structure of thermodynamics". *Surf. Sci.*, **613**, 1234–1248.
- 14 Ibach, H. (1997) The role of surface stress in reconstruction, epitaxial growth and stabilization of mesoscopic structures. *Surf. Sci. Rep.*, **29**, 195–263.
- 15 Yang, Z., Wang, Z., and Zhao, Y. (2008) Surface stress induced by adatoms on solid surfaces. *Int. J. Nonlinear Sci. Numer. Simul.*, **9**, 323–329.
- 16 Stoney, G. (1909) The tension of metal films deposited by electrolysis. *Proc. R. Soc. Lond. A*, **82**, 172.
- 17 Freund, L., Floro, J., and Chason, E. (1999) Extension of the Stoney formula for substrate curvature to configurations with thin substrates and large deformations. *Appl. Phys. Lett.*, **74**, 1987–1991.
- 18 Sander, D., Schmidthals, C., Enders, A., and Kirschner, J. (1998) Stress and structure of Ni monolayers on W(110): the importance of lattice mismatch. *Phys. Rev. B*, **57**, 1406.
- 19 Bar, B., Altus, E., and Tadmor, E. (2010) Surface effects in non-uniform nanobeams: continuum vs. atomistic modelling. *Int. J. Solids Struct.*, **47**, 1243–1252.
- 20 Sanfeld, A. (1987) Sur quelques difficultés conceptuelles relatives à la tension de surface des solides. *J. Chimie. Phys.*, **84**, 12–15.
- 21 Cahn, J. and Larché, F. (1982) Surface stress and the chemical equilibrium of a small crystal. II. Solid particles embedded in a solid matrix. *Acta Metall.*, **30**, 51–56.
- 22 Steigman, D. and Ogden, R. (1999) Elastic surface–substrate interactions. *Proc. R. Soc. Lond. A*, **455**, 437–474.
- 23 Gurtin, M. and Murdoch, A. (1975) A continuum theory of elastic material surfaces. *Arch. Ration. Mech. Anal.*, **57**, 291–323.
- 24 Gurtin, M. and Murdoch, A. (1975) Addenda to our paper: a continuum theory of elastic material surfaces. *Arch. Ration. Mech. Anal.*, **59**, 389–390.
- 25 Gurtin, M. and Murdoch, A. (1978) Surface stress in solids. *Int. J. Solids Struct.*, **14**, 431–440.
- 26 Kern, R. and Müller, P. (1997) Elastic relaxation of coherent epitaxial deposits. *Surf. Sci.*, **392**, 103–133.
- 27 Dingreville, R., Qu, J., and Cherkaoui, M. (2005) Surface free energy and its effect on the elastic behavior of nano-sized particles, wires and films. *J. Mech. Phys. Solids*, **53**, 1927–1854.
- 28 de Planta, T., Ghez, R., and Piaz, F. (1964) On surface stress of small particles. *Helv. Phys. Acta*, **47**, 74–81.

- 29 Vermaak, J.S., Mays, C.W., and Kuhlman-Wilsdorf, D. (1968) On surface stress and surface tension. *Surf. Sci.*, **12**, 128–135.
- 30 Solliard, C. and Flueli, M. (1985) Surface stress and size effect on the lattice parameter in small particles of gold and platinum. *Surf. Sci.*, **156**, 487–494.
- 31 Jiang, Q., Liang, L., and Zhao, D. (2001) Lattice contraction and surface stress of fcc nanocrystals. *J. Phys. Chem. B*, **105**, 6276–6281.
- 32 Streitz, F., Cammarata, R., and Sieradzki, R. (1994) Surface stress effects on elastic properties. I. Thin metal films. *Phys. Rev. B*, **49**, 10699–10705.
- 33 Zhang, T., Wan, Z., and Chan, W. (2010) Eigenstress model for surface stress of solids. *Phys. Rev. B*, **81**, 195427.
- 34 He, L., Lim, C., and Wu, B. (2004) A continuum model for size-dependent deformation of elastic films of nano-scale thickness. *Int. J. Solids Struct.*, **41**, 847–857.
- 35 Lim, C. and He, L. (2004) Size-dependent nonlinear response of thin elastic films with nano-scale thickness. *Int. J. Mech. Sci.*, **46**, 1715–1726.
- 36 Duan, H., Wang, J., Huang, Z., and Karihaloo, B. (2005) Size-dependent effective elastic constants of solids containing nano-inhomogeneities with interface stress. *J. Mech. Phys. Solids*, **53**, 1574.
- 37 Lu, P., He, L., Lee, H., and Lu, C. (2006) Thin plate theory including surface effects. *Int. J. Solids Struct.*, **43**, 4631–4647.
- 38 Huang, D. (2008) Size-dependent response of ultra-thin films with surface effects. *Int. J. Solids Struct.*, **45**, 568–579.
- 39 Dingreville, R. and Qu, J. (2008) Interfacial excess energy, excess stress and excess strain in elastic solids: planar interfaces. *J. Mech. Phys. Solids*, **56**, 1944–1954.
- 40 He, J. and Lilley, C. (2008) Surface effect on the elastic behaviour of static bending nanowires. *Nano Lett.*, **8**, 1798–1802.
- 41 Guo, J. and Zhao, Y. (2005) The size-dependent elastic properties of nanofilms with surface effects. *J. Appl. Phys.*, **98**, 074306.
- 42 Zhao, X. and Rajapaske, R. (2009) Analytical solutions for a surface-loaded isotropic elastic layer. *Int. J. Eng. Sci.*, **47**, 1433–1444.
- 43 Lu, C., Lim, C., and Chen, W. (2009) Size-dependent elastic behaviour of FGM ultra-thin films based on generalised refined theories. *Int. J. Solids Struct.*, **46**, 1176–1194.
- 44 Gurtin, M., Markenscoff, X., and Thurston, R. (1976) Effect of surface stress on the natural frequency of thin crystals. *Appl. Phys. Lett.*, **29**, 529–532.
- 45 Ricci, A. and Ricciardi, C. (2010) A new finite element approach for studying the effect of surface stress on microstructures. *Sens. Actuators A Phys.*, **159**, 141–148.
- 46 Cuenot, S., Frétiqny, C., Dumoustier-Champagne, S., and Nysten, B. (2004) Surface tension effect on the mechanical properties of nanomaterials measured by atomic force microscopy. *Phys. Rev. B*, **69**, 165410.
- 47 Kis, A., Kasas, S., Babic, B., Julij, A., Benoit, W., Briggs, G., Schönenberger, C., Catsicas, S., and Forr, L. (2002) Nanomechanics of microtubes. *Phys. Rev. Lett.*, **89**, 248101.
- 48 Chen, C., Shi, Y., Zhang, Y., and Yan, Y. (2006) Size-dependence of Young's modulus in ZnO nanowires. *Phys. Rev. Lett.*, **96**, 075505.
- 49 Liang, H., Upmanyu, M., and Huang, H. (2005) Size-dependent elasticity of nanowires: nonlinear effects. *Phys. Rev. B*, **71**, 241403.
- 50 Wang, Z., Zhao, Y., and Huang, Z. (2010) The effects of surface tension on the elastic properties of nanostructures. *Int. J. Eng. Sci.*, **48**, 140–150.
- 51 Shim, S., Bei, H., Killer, M., Pharr, G., and George, E. (2009) Effects of focused ion beam milling on the compressive behaviour of directionally solidified micropillars and the nanoindentation response of an electropolished surface. *Acta Mater.*, **57**, 503.
- 52 Kiener, D., Grosinger, W., Dehm, G., and Pippan, R. (2008) A further step towards an understanding of size-dependent crystal plasticity: *in situ* tension experiments of miniaturized single-crystal copper samples. *Acta Mater.*, **56**, 580.
- 53 Uchic, M., Dimiduck, D., Florando, J., and Nix, W. (2004) Sample dimensions influence strength and crystal plasticity. *Science*, **305**, 985–988.

- 54 Ying, G., Duan, H., Sun, X., Zhang, Z., Xu, J., Li, Y., Wang, J., and Yu, D. (2006) Surface effects on elastic properties of silver nanowires: contact atomic-force microscopy. *Phys. Rev. B*, **73**, 235409.
- 55 Stan, G., Ciobanu, C., Parthangal, P., and Cook, R. (2007) Diameter-dependent radial and tangential elastic moduli of ZnO nanowires. *Nano Lett.*, **7**, 3691–3695.
- 56 Nam, C., Jaroenapibal, P., Tham, D., Luzzi, D., Evoy, S., and Fisher, J. (2006) Diameter-dependent electrochemical properties of GaN nanowires. *Nano Lett.*, **6**, 153–157.
- 57 Zhu, Y., Xu, F., Qin, Q., Fung, W., and Lu, W. (2009) Mechanical properties of vapour–liquid synthesized silicon nanowires. *Nano Lett.*, **9**, 3934–3938.
- 58 Agrawai, R., Peng, B., Gdoutos, E., and Espinosa, H. (2008) Elasticity size effects in ZnO nanowires: a combined experimental–computational approach. *Nano Lett.*, **8**, 3668–3672.
- 59 Gordon, M., Baron, T., Dhalluin, F., Gentile, P., and Ferret, P. (2009) Size effects in mechanical deformation and fracture of cantilevered silicon nanowires. *Nano Lett.*, **9**, 525–529.
- 60 Heidelberg, A., Ngo, L., Wu, B., Phillips, M., Sharma, S., Kamins, T., Sader, J., and Boland, J. (2006) A generalized description of the elastic properties of nanowires. *Nano Lett.*, **6**, 1101–1105.
- 61 Park, H. and Klein, P. (2008) Surface stress effects on the resonant properties of metal nanowires: the importance of finite deformation kinematics and the impact of residual surface stress. *J. Mech. Phys. Solids*, **56**, 3144–3166.
- 62 Portales, H., Goubet, N., Saviot, L., Aditchev, S., Murray, D., Mermert, A., Duval, E., and Pileni, M. (2008) Probing atomic ordering and multiple twinning in metal nanocrystals through their vibrations. *PNAS*, **105**, 14784.
- 63 Ikezawa, M., Okuno, T., and Masumoto, Y. (2001) Complementary detection of confined acoustic phonons in quantum dots by coherent phonon measurement and Raman scattering. *Phys. Rev. B*, **64**, 201315(R).
- 64 Chen, Q., Shi, Y., Zhang, Y., Zhu, J., and Yan, Y. (2006) Size dependent of Young modulus in ZnO nanowires. *Phys. Rev. Lett.*, **96**, 175505.
- 65 Li, X. and Peng, X. (2008) Theoretical analysis of surface stress for a microcantilever with varying widths. *J. Phys. D Appl. Phys.*, **41**, 065301.
- 66 Sun, C. and Zhang, H. (2003) Size-dependent elastic moduli of platelike nanomaterials. *J. Appl. Phys.*, **93**, 1212–1215.
- 67 Deng, X., Joseph, V., Mai, W., Wang, Z., and Wu, C. (2009) Statistical approach to quantifying the elastic deformation of nanomaterials. *Proc. Natl. Acad. Sci. USA*, **106**, 11845–11850.
- 68 Guo, J. and Zhao, Y. (2005) The size-dependent elastic properties of nanofilms with surface effects. *J. Appl. Phys.*, **98**, 074306.
- 69 Lim, C. (2010) On the truth of nanoscale for nanobeams based on nonlocal elastic stress field theory: equilibrium, governing equation and static deflection. *Appl. Math. Mech. Eng. Ed.*, **31**, 37–54.
- 70 Glas, F. (2006) Critical dimensions for the plastic relaxation of strained axial heterostructures in free-standing nanowires. *Phys. Rev. B*, **74**, 121302.
- 71 Schmidt, V., McIntyre, P., and Gösele, U. (2008) Morphological instability of misfit-strained core–shell nanowires. *Phys. Rev. B*, **77**, 235302.
- 72 Colin, J., Grilhe, J., and Müller, P. (2009) Nanostructures instabilities induced by anisotropic epitaxial stress. *Phys. Rev. E*, **80**, 052601.